Available online at www.sciencedirect.com
SCIENCE DIRECT®
Journal of Catalysis 242 (2006) 172–183
JOURNAL OF CATALYSIS
www.elsevier.com/locate/jcat

Modifications of the elementary steps involved in the O_2-oxidation of the adsorbed CO species over Pt/Al_2O_3 by co-adsorbed NO species

Salim Derrouiche, Daniel Bianchi *

Laboratoire d'Application de la Chimie à l'Environnement (LACE), UMR 5634, Université Claude Bernard, Lyon-I, Bat. Raulin, 43 Bd du 11 Novembre 1918, 69622 Villeurbanne, France

Received 31 January 2006; revised 4 June 2006; accepted 8 June 2006

Available online 11 July 2006

Abstract

The study concerns modifications of the elementary steps involved in the isothermal oxidation with O_2 of linear and bridged CO species adsorbed on a reduced 2.9% Pt/Al_2O_3 catalyst in the presence of co-adsorbed N-containing species. The rate of the CO_2 production at $T < 350$ K: $RCO_2(t)$ with time on stream, t, in $x\%$ $O_2/y\%$ Ar/He ($x, y < 3$) presents a decreasing exponential-like profile for a Pt dispersion $D < 0.26$ in the absence of N-containing species. This profile is significantly modified if NO is adsorbed before oxidation of the adsorbed CO species. An induction period is observed, with a characteristic peak defined by the coordinates of its maximum, t_m and $RCO_{2\,m}$. This new $RCO_2(t)$ profile is unchanged during successive reduction in CO/oxidation in O_2 cycles, indicating that the perturbation created by the NO adsorption is permanent at $T < 350$ K. The impact of NO adsorption on $RCO_2(t)$ is ascribed to N_{ads} species formed by NO dissociation. Previous studies allow us to show that the modification of the $RCO_2(t)$ profile is due to the decreased rate constants of two elementary steps after the adsorption of NO: (a) the desorption of the bridged CO species, which leads to fewer Pt° sites for the activation of oxygen, and (b) the Langmuir–Hinshelwood steps involved in the oxidation of the adsorbed CO species.

Keywords: CO/O_2 reaction; Pt/Al_2O_3; Adsorbed CO species; Co-adsorbed NO species; Isothermal oxidation; Kinetic model and microkinetics

1. Introduction

The aim of the microkinetic approach [1] of a gas/solid catalytic reaction is to correlate the kinetic parameters of the surface elementary steps (i.e., adsorption, desorption, Langmuir–Hinshelwood steps) involved in a plausible kinetic model of the reaction to the turnover frequency (TOF) for different experimental conditions. Different approaches can be followed for characterizing the elementary steps, including DFT calculations and experimental procedures on either well-defined single-crystal surfaces or conventional metal-supported catalysts. In previous studies [2–8], this latter approach has been developed for the CO/O_2 reaction on reduced Pt/Al_2O_3 catalysts, taking into particular account the presence of different adsorbed CO species on the Pt° sites (i.e., linear, bridged, and threefold-coordinated CO species) [7,8]. It has been shown that the evolution of TOF during lighting-off tests can be reasonably interpreted considering that the strongly adsorbed linear CO species (which is the main adsorbed CO species on Pt/Al_2O_3) is the intermediate of the reaction [4,6]. The bridged CO species is weakly adsorbed [8], and its removal from the surface (by either the modification of the adsorption equilibrium or the oxidation with O_2) provides Pt° sites for the activation of a weakly adsorbed oxygen species involved in the oxidation of the linear CO species at low temperatures [2,3]. The experimental microkinetic approach allows us to correlate modifications of the TOF of the CO/O_2 reaction through changes in catalyst preparation, such as Pt dispersion D [9–11] and the nature of the support [12], to the modifications of the kinetic parameters of specific elementary steps. This constitutes a concretization of a perspective imagined by Boudart in the Foreword of [1] and extended in [13]: the microkinetic as a tool to aide catalyst development. For instance, literature data indicate that the TOF of the CO/O_2 reaction decreases with increasing Pt particle size [14]. It has been shown [9–11] that this is related to the fact that

* Corresponding author.
E-mail address: daniel.bianchi@univ-lyon1.fr (D. Bianchi).

0021-9517/$ – see front matter
doi:10.1016/j.jcat.2006.06.006

the increase in D (a) decreases the rate constant of oxidation of the linear CO species at low temperatures and (b) augments the heat of adsorption of the bridged CO species (denoted by $E_{B\theta B}$ at a coverage θ_B), limiting the amount of Pt° sites for the activation of oxygen. Finally, experimental microkinetic study [2–8] of the CO/O_2 reaction on Pt/Al_2O_3 has focused on the fact that two types of Pt° sites (in significantly different amounts) are involved in the CO/O_2 reaction at low temperatures on Pt/Al_2O_3; roughly 90% of the Pt° sites adsorb the linear CO species, and the remaining fraction (10%) adsorbs the bridged CO species and the weakly adsorbed oxygen species. This competitive chemisorption bridged CO/oxygen species on a small number of Pt° sites constitutes a key process of the CO/O_2 reaction on Pt/Al_2O_3. Characterizing these sites constitutes one of the difficulties of the experimental microkinetic approach of the CO/O_2 reaction. This justifies the development of experimental procedures associated with kinetic models to confirm the impact of these Pt° sites on the rate of the CO/O_2 reaction. For instance, we have explained how modifying the properties of these two types of Pt° sites with Pt dispersion affect the TOF of the CO/O_2 reaction by studying the isothermal oxidation of the linear and bridged CO species on Pt/Al_2O_3 catalysts [10,11].

In the present article, which is an extension of [11], we confirm the important role of the small amount of Pt° sites adsorbing the bridged CO species and the weakly adsorbed oxygen species by studying the impact of co-adsorbed NO species on the rate of O_2 oxidation of the linear and bridged CO species. This is of particular interest in light of the reactions involved in three-way catalysis and De-NO_x on Pt-containing catalysts.

2. Experimental

2.1. Catalysts

The 2.9 wt% Pt/Al_2O_3 catalyst and the reduction procedure by hydrogen at 713 K was the same as used in previous studies [2–11]. The Pt dispersion was decreased to low values ($D < 0.26$) according to the following procedure [11]: After reduction of the catalyst, CO was adsorbed at 300 K using the switch He → 2% CO/2% Ar/He, followed by a temperature increase (at 10 K/min) to 713 K. At 713 K, the catalyst was treated in O_2 for 10 min and then in H_2 for 30 min, providing a Pt dispersion D in the range of 0.5–0.6. Then the subsequent O_2 and H_2 pretreatments at 713 K performed before each experiment decreased D very progressively. In the present study, the 2.9% Pt/Al_2O_3 catalyst sample was used in numerous transient experiments using CO/(and/or O_2)/He gas mixtures, leading to a Pt dispersion in the 0.2–0.26 range measured by CO chemisorption at 300 K [10].

2.2. Analytical procedures for studying the elementary steps

The two analytical systems used in the present study have been described in detail elsewhere [2–11]. Mainly, they allowed us to perform experiments in the transient regime studying the evolutions either of the molar fractions of the gas at the outlet of a quartz microreactor (weight of catalyst = 0.2 g) with a quadrupole mass spectrometer or the IR bands of the adsorbed species using a stainless steel IR cell with a FTIR spectrometer. The first analytical system was used to determine the rate of CO_2 production, $RCO_2(t)$, during isothermal oxidation of the adsorbed CO species at $T_O < 350$ K, according to the following switches (100 cm^3/min): He (last stage of the pretreatment procedure) → 1% CO/1% Ar/He (CO adsorption, duration t_a) → He (desorption of a fraction of the bridged CO species, duration t_d) → x% O_2/y% Ar/He (isothermal oxidation of the linear CO species and of the remaining fraction of the bridged CO species, duration t_O, $x, y < 4$). During the oxidation stage, strongly adsorbed oxygen species were formed in parallel to the removal of linear CO species by oxidation [5]. These species were reduced at $T < 350$ K by CO, according to the following switches: x% O_2/y% Ar/He (formation of the adsorbed oxygen species) → He, t_d → 1% CO/1% Ar/He (reduction of the oxygen species, duration t_r). The reduction stage was associated with the adsorption of CO as linear and bridged CO species [5]. This allowed us to perform successive isothermal oxidation/reduction of the adsorbed species, which we call O/R cycles [5].

The present study aimed to investigate the impact of NO adsorption before the oxidation stage according to such switches as 1% CO/1% Ar/He → He → 1% NO/1% Ar/He → He → x% O_2/y% Ar/He. The dispersion of Pt was measured using either CO or O_2 chemisorption at 300 K [10] after each reduction pretreatment. The experiments were designed according to several criteria to prevent the contribution of diffusion processes on the measurement of $RCO_2(t)$ [11]. The mass spectrometer did not allow us to quantify CO_2 and N_2O individually for experimental conditions leading to their simultaneous production. For these situations, we quantified the $m/e = 44$ signal as CO_2.

The second analytical system with a FTIR spectrometer as a detector [2,7,9] allowed us to perform similar transient experiments studying the evolutions of the IR bands of the adsorbed species. The solid was compressed to form a disk ($\Phi = 1.8$ cm, $m = 40$–100 mg), which was placed in the sample holder of a small-internal volume stainless steel IR cell (transmission mode). To prevent a significant difference in the Pt dispersion of the sample between the two analytical systems, the pellet for the IR study was prepared with the catalyst sample previously used with the quartz microreactor (last measurement of D: 0.20).

3. Results

3.1. Design of the experimental microkinetic procedure

In a previous study [11], it was shown that the rate of the CO_2 production, $RCO_2(t)$, at $T < 350$ K during O_2 oxidation of adsorbed CO species on Pt/Al_2O_3 catalysts was the sum of the rates of oxidation of the linear and of the bridged CO species remaining on the Pt° sites after desorption in helium: $RCO_2L(t)$ and $RCO_2B(t)$, respectively. The $RCO_2(t)$ curves present different profiles according to the Pt dispersion [10,11]. For $D \lessapprox 0.6$, a decreasing exponential-like profile was observed, whereas for $D \gtrapprox 0.6$, $RCO_2(t)$ was characterized by an induction period ending with a peak defined by the coordinates of it maximum, t_m and $RCO_{2\,m}$ [11]. The amount of CO_2 associated with the $RCO_2(t)$ peak indicates clearly that this peak was due mainly to oxidation of the linear CO species, whereas oxidation of the bridged CO species is involved in the induction period [10,11]. Several reports have noted the presence of an induction period for the oxidation of adsorbed CO species on Pt- and Pd-supported catalysts [15–17]. A kinetic model has been developed to interpret the experimental data considering that the induction period is linked to the increased number of Pt° sites activating the weakly adsorbed oxygen species by oxidation of the bridged CO species [11]. This model provides mathematical expressions of the coordinates of the maximum of $RCO_2L(t)$ that are dependent on several kinetic parameters [11]:

$$t_m = \left(\frac{1}{k_{OB}x\mathrm{NT_B}\sqrt{K_{O_2}P_{O_2}}}\right)\ln\left[\left(\frac{B(0)}{\mathrm{NT_B}-B(0)}\right)\frac{k_{OB}}{k_3}\right], \quad (1)$$

$$RCO_2L_m = k_{OB}L(0)x\mathrm{NT_B}\left(\frac{\mathrm{NT_B}}{B(0)}\right)^{k_3/k_{OB}} \times \left(\frac{k_3}{k_{OB}+k_3}\right)^{(k_3/k_{OB})+1}\sqrt{K_{O_2}P_{O_2}}, \quad (2)$$

where k_{OB} (k_3), $\mathrm{NT_B}$ ($\mathrm{NT_L}$), and $B(0)$ ($L(0)$) are related to the bridged (linear) CO species, the rate constant of oxidation of the L–H step, the total amount (in molecules/cm^2) of Pt° sites that may adsorb the species, and the amount of CO species at $t = 0$ of oxidation, respectively; K_{O_2} and P_{O_2} are the adsorption coefficient and the partial pressure of oxygen, respectively; and x is the number of Pt° sites for the adsorption of oxygen created by the removal of each bridged CO species [11]. The linear CO species is strongly adsorbed [7,8], leading to $L(0) = \mathrm{NT_L}$, whereas $B(0) \leqslant \mathrm{NT_B}$ because a fraction of the bridged CO species desorbs during the helium purge before oxidation. Expression (1) shows that a CO_2 peak can be observed ($t_m > 0$) only if

$$B(0) \geqslant \frac{\mathrm{NT_B}}{\frac{k_{OB}}{k_3}+1}. \quad (3)$$

Otherwise, the rate of CO_2 production is the greatest at time 0 of oxidation, leading to a decreasing exponential-like profile (situation observed for $D \lessapprox 0.6$ [10,11]). The value of $B(0)$ is dependent on (a) the activation energy of desorption of the bridged CO species and (b) the duration of the isothermal desorption t_d before the oxidation. It has been shown [8] that the activation energy of desorption of the bridged CO species increases linearly with the decrease in its coverage θ_B whatever the Pt dispersion. This explains why a fraction of the bridged CO species remains adsorbed after desorption duration t_d. However, the activation energy of desorption for $\theta_B = 1$ increases from 46 kJ/mol at $D \lessapprox 0.5$ to 57 kJ/mol at $D = 0.8$ [10]. This explains why the higher the Pt dispersion, the higher the $B(0)$ value, allowing the criterion (3) to be fulfilled.

In the present study we selected a catalyst with a low Pt dispersion, which leads to an exponentially decreasing profile for $RCO_2(t)$ at 300 K < T < 350 K after a desorption duration of $t_d = 80$ s before oxidation [10,11]. The aims of the present experimental microkinetic study were to investigate how this profile is modified by co-adsorbed N-containing species. This leads us to study the competitive chemisorption between adsorbed CO and NO species in a first step.

3.2. *Competitive chemisorption CO–NO using FTIR spectroscopy*

3.2.1. *Impact of the adsorption of CO on the adsorbed NO species*

The adsorption of 1% NO/He at 300 K for 5 min on the freshly reduced 2.9% Pt/Al_2O_3 catalysts with $D = 0.2$ leads to spectrum a in Fig. 1A showing a main IR band at 1705 cm^{-1}

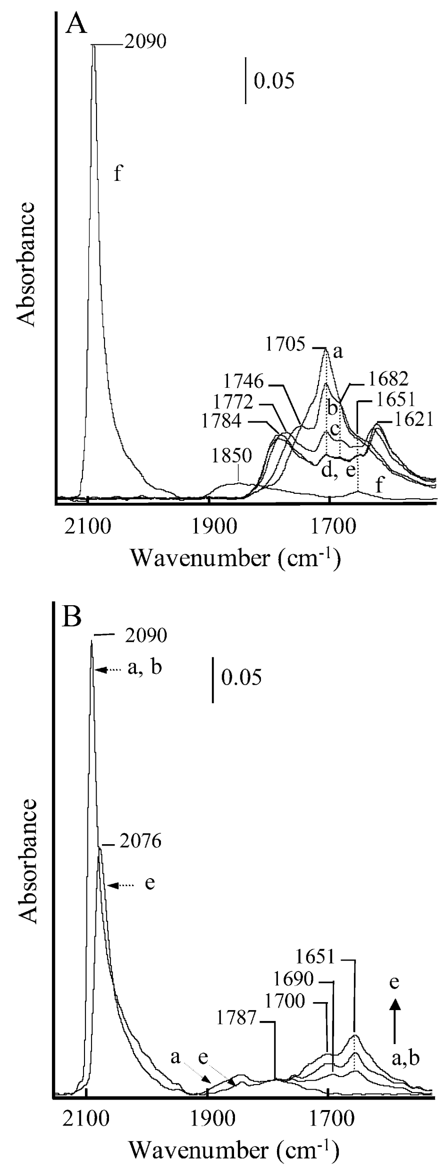

Fig. 1. Competitive chemisorption between CO and NO on 2.9% Pt/Al_2O_3 ($D \approx 0.20$) at 300 K studied by FTIR spectroscopy. (A) Adsorption of CO on the strongly adsorbed NO species: (a) in the presence of 1% NO/He; (b–e) desorption in helium 10, 20, 35, and 80 s, respectively; (f) after 10 s of adsorption of 1% CO/He. (B) Adsorption of NO on the strongly adsorbed CO species: (a) 5 min in helium after adsorption of 1% CO/He; (b–e) time on stream in 1% NO/He 15, 55, 150, and 380 s, respectively.

Table 1
IR bands observed on the Pt particles of the reduced 2.9% Pt/Al_2O_3 solid with a Pt dispersion $D \approx 0.2$

Experimental conditions	Position (cm^{-1}) and intensity	Assignment (* references)
Adsorption of NO at 300 K	1705 (s)	Linear NO*
	1764 (w)	Linear NO*
	1651 (w)	Bridged NO
Adsorption of CO at 300 K	2090 (v.s)	Linear CO**
	1845 (w)	Bridged CO**
Co-adsorption of CO and NO at 300 K	2090 (v.s)	Linear CO
	1845 (w)	Bridged CO
Co-adsorption of CO and NO at 300 K followed TPSR at $T > 350$ K	2090 (v.s)	Linear CO
	1845 (w)	Bridged CO
	2257 (v.w)	Isocyanate (on Al_2O_3)***
	2233 (v.w)	Isocyanate (on Pt° or Al_2O_3)***

Note. (v.s), (s), (v.w), and (w): very strong, strong, very weak, and weak.
* [18] and references therein, ** [7,8] and references therein, *** [19,43,44].

associated with shoulders at 1746 and 1651 cm^{-1}. This spectrum is similar to that obtained on the same catalyst for a higher D value with IR bands at 1710 and 1764 cm^{-1} [18]. According to literature data (see references in [18]), the IR bands at 1710/1705 cm^{-1} and 1764/1746 cm^{-1} can be ascribed to linear NO species adsorbed on terrace and defect Pt sites, respectively, whereas the shoulder at 1651 cm^{-1} must correspond to a bridged NO species not observed at a higher Pt dispersion [18]. Several IR bands (not shown) of low intensities can be seen in the 1600–1200 cm^{-1} range, including 1227, 1430, and 1480 cm^{-1}, ascribed either to nitrito-, nitro-, and nitrato-species on the Al_2O_3 support (denoted by NO_x–Al_2O_3) [19] or to bent NO species on Pt° sites (IR band at 1430 cm^{-1}) (see references in [18]). The desorption in helium led to progressive modification of the IR bands (Fig. 1A, spectra a–e); the IR band at 1705 cm^{-1} decreased progressively and split into two new IR bands at 1784 and 1621 cm^{-1} with a shoulder at 1682 cm^{-1}. The reintroduction of 1% NO/He provided a spectrum identical to spectrum a in Fig. 1A. The evolution during helium desorption may be due to the removal of a weakly adsorbed NO species interacting with the strongly adsorbed NO species. Recent IRAS literature data on single Pt crystals [20,21] supported by DFT calculations [21,22] attributed the complexity of the IR spectra of the adsorbed NO species to (a) the unpaired electron in the antibonding $2\pi^*$ orbital of NO, which permits formation of a wide variety of linear and bridged NO species according to the position of the Pt° sites, and (b) interconversion of the bridged NO species (the most stable NO species at low coverage) into the linear NO species with the increase in coverage. After the adsorption of NO, a switch He → 1% CO/He led to disappearance of the IR bands of the adsorbed NO species associated with the detection of (a) a sharp IR band at 2090 cm^{-1} and (b) a broad IR band in the 1900–1700 cm^{-1} range, indicating the formation of the linear and bridged CO species, respectively [8]. The IR bands below 1600 cm^{-1} ascribed to NO_x–Al_2O_3 species were not affected by CO adsorption. The presence of the IR band at 1651 cm^{-1} in spectrum f, associated with IR bands at 1440 and 1229 cm^{-1} (not shown), indicates the formation of carbonate species on the support. The displacement at 300 K of the molecularly adsorbed NO species by the adsorbed CO species is consistent with the observations on Pt(100) [23,24]. Table 1 summarizes the IR band positions of the adsorbed species on the Pt particles and their assignments.

3.2.2. *Impact of NO adsorption on the adsorbed CO species*

Spectrum a in Fig. 1B was recorded after the adsorption of 1% CO/He on the reduced 2.9% Pt/Al_2O_3 solid ($D \approx 0.20$), followed by a helium purge for 5 min. The sharp IR band at 2090 cm^{-1} and the weak and broad IR band in the 1900–1700 cm^{-1} range can be ascribed to the linear CO species on Pt° sites and to the bridged CO species remaining on the surface after the desorption at 300 K, respectively [8]. The intensity of the IR band of the bridged CO species was very low, providing only semiquantitative data during the different experiments. The position of the IR band of the linear CO species was higher than that observed for $D = 0.44$: 2073 cm^{-1} [9] because of the impact of the average particle size on this parameter [9,25]. There were no significant modifications of the IR bands of the adsorbed species after 10 s of the switch He → 1% NO/He (Fig. 1B, spectrum b), in agreement with IRAS observations on Pt(100) [23,24]. This indicates that the competitive chemisorption CO–NO was in favor of CO. Fig. 1B shows that for longer time on stream in 1% NO/He, (a) the IR bands of the linear and bridged CO species decreased progressively (compare spectra a and e), associated with a shift of the IR band of the linear CO species (from 2090 to 2076 cm^{-1} after 380 s in 1% NO/He), and (b) in parallel, strongly overlapped IR bands increased at 1700 and 1651 cm^{-1} (Fig. 1B) and at 1440 and 1229 cm^{-1} (not shown). The IR bands at 1651, 1440, and 1229 cm^{-1} indicate the formation of different carbonates species on the alumina support because of the adsorption of CO_2 [10,26] formed by slow oxidation of the adsorbed CO species with time on stream in 1% NO/He. This leads to the conclusion that there was a small number of free Pt° sites at time 0 of NO introduction for the activation of NO, probably those released by the desorption of a fraction of the bridged CO species. The IR band at 1700 cm^{-1} in spectrum e in Fig. 1B (observed at 1690 cm^{-1} in spectrum c) indicates the formation of a linear NO species on the Pt° sites [18] released by the oxidation of the linear CO species. This oxidation suggests that dissociation of NO occurred at 300 K. On Pt single crystals [27], the dissociation seems favored by specific defect sites, such as on Pt(410) [28,29], Pt(211), and Pt(411) [30,31]. On Pt/SiO_2, Morrow et al. [32] reported a slight NO dissociation at 300 K and assigned an IR band at 1710 cm^{-1} to a linear NO species on a partially oxidized Pt surface. Finally, the adsorption of NO in the presence of adsorbed CO species may lead to a Pt surface containing (a) molecularly adsorbed NO species (i.e., the linear NO species with an IR band at $\approx$1700 cm^{-1}), (b) N_{sads} and O_{sads} species from the NO dissociation, and (c) the remaining fraction of the adsorbed CO species. Compared with a previous study, Fig. 1B shows that the rate of oxidation of the linear CO species using 1% NO/He was much less than that observed with 1% O_2/He [2]. This is probably linked to the dissociation energies of the O-containing gases used in the present study: 498, 630, and 1076 kJ/mol for O_2, NO, and CO, respectively [33].

3.2.3. Co-adsorption and reaction of NO/CO at $T < 350$ K

The introduction of 0.5% CO/0.5% NO/He on Pt/Al_2O_3 at 300 K led in the 1700–2100 cm^{-1} range to the same spectrum as that after the adsorption of 1% CO/He (spectrum a in Fig. 1B). However, strong IR bands at 1651, 1440, and 1229 cm^{-1} can be ascribed to carbonate species on the support, indicating the oxidation of CO by oxygen species coming from the NO dissociation via a molecularly adsorbed NO species not detected by FTIR (either present in small amounts or inactive in IR such as the adsorption of NO parallel to the surface). The IR bands of isocyanate species at 2251 and 2235 cm^{-1} [19] were detected only at a reaction temperature of 360 K. The presence of a small amount of free Pt° sites for the dissociation of NO (without detectable molecularly adsorbed NO species) is consistent with IRAS observations on Pt(100); the adsorption of a CO/NO mixture (total pressure 8×10^{-7} mbar, $P_{NO}/P_{CO} = 1.5$) led only to the IR bands of the linear and bridged CO species, whereas a small rate of CO_2 production was observed [23].

3.3. Competitive chemisorption CO–NO using MS

3.3.1. Adsorption of NO on the adsorbed CO species

Fig. 2A shows the evolution of the molar fractions of the gases at the outlet of the quartz microreactor during the switch He → 1% CO/1% Ar/He at 300 K on the reduced 2.9% Pt/Al_2O_3 catalyst. The amount of adsorbed CO species at 300 K, $QCO_{ads} = 39$ µmol/g ($D \approx 0.26$), was obtained using the difference between the argon and the CO curves [3]. After a helium purge (Fig. 2B), a new switch, He → 1% CO/1% Ar/He at 300 K, was performed (Fig. 2C) to quantify the amount of reversible adsorbed CO species: $QCO_{wads} = 5$ µmol/g (a fraction of the bridged CO species on Pt and of the weakly adsorbed CO species on the $Al^{+\delta}$ sites of the support [2,3]). The amount of strongly adsorbed CO species, corresponding mainly to the linear CO species, was $QCO_{sads} = 34$ µmol/g. After a helium purge (Fig. 2D), a 1% NO/1% Ar/He mixture was introduced (Fig. 2E), leading to (a) the absence of CO desorption and (b) a NO consumption, $QNO_{ads} = 33$ µmol/g, associated with detection of small amounts of CO_2 or/and N_2O ($m/e = 44$ quantified as CO_2). These observations show that (a) NO did not displace CO, in agreement with Fig. 1, and (b) NO was dissociated on the free Pt sites due to desorption of the bridged CO species and consumption by the oxygen species of the adsorbed CO species, explaining the formation of CO_2 and/or N_2O (Fig. 2E). These observations are consistent with the decreased IR band of the linear CO species and the formation of carbonate on the support shown in Fig. 1B. A fraction of the NO consumption is due to (a) adsorption of the strongly adsorbed linear NO species, in parallel to oxidation of the adsorbed CO species (Fig. 1A), and (b) formation of the NO_x–Al_2O_3 species.

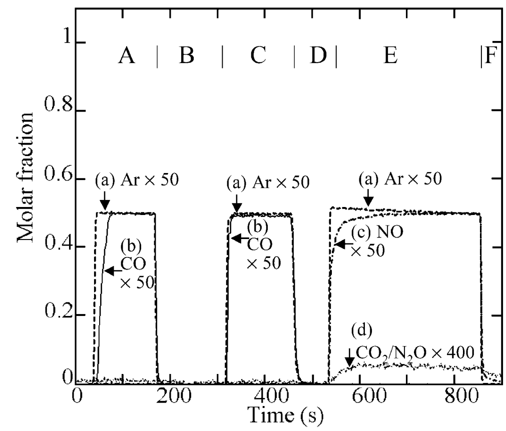

Fig. 2. Competitive chemisorption between adsorbed CO species on 2.9% Pt/Al_2O_3 and NO_g at 300 K studied by MS. (A, C) Adsorption of 1% CO/1% Ar/He; (B, D, F) desorption in helium; (E) adsorption of 1% NO/1% Ar/He.

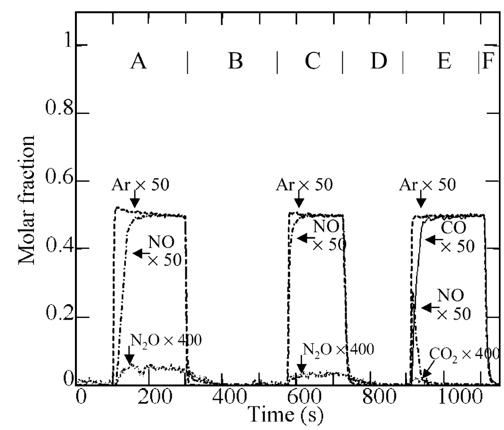

Fig. 3. Competitive chemisorption between adsorbed NO species on 2.9% Pt/Al_2O_3 and CO at 300 K studied by MS. (A, C) Adsorption of 1% NO/1% Ar/He; (B, D, F) desorption in helium; (E) adsorption of 1% CO/He.

3.3.2. Adsorption of CO on the adsorbed NO species

Fig. 3A shows the evolution of the molar fractions of the gases during the switch He → 1% NO/1% Ar/He at 300 K on the freshly reduced 2.9% Pt/Al_2O_3 catalyst. The amount of adsorbed NO species was $QNO_{ads} = 53$ µmol/g. A small amount of N_2O production ($m/e = 44$) occurred, according to the global reaction

$$2NO \rightarrow N_2O + O_{sads}. \quad (4)$$

The NO conversion was ≈1%, and this value decreased with time on stream, indicating that the N_2O production was not sustained. A similar low N_2O production during the adsorption of NO at 300 K on Pt/Al_2O_3 catalysts was reported by Maunula et al. [34]. On Pt single crystals, N_2O formation from adsorbed NO species is often observed at higher temperatures ($T > 400$ K), indicating a significant activation energy for the catalytic processes [30]. However, Burch et al. [35,36] showed, based on DFT calculations, that there are two possible routes for the N_2O formation: NO dissociation and decomposition of an adsorbed dimer $(NO_{ads})_2$ on the Pt defect sites. These authors concluded that the dimer mechanism has a very low activation energy, explaining that N_2O can be formed at low temperatures on several metal surfaces. The involvement of defect Pt sites explains why this reaction is absent on well-defined Pt single crystals. Moreover on Pt(100), some authors [37] used DFT calculations to show that recombination of the N_{ads} species to form N_2 is a barrierless process, suggesting that the N_2O formation via the NO dissociation is not significant due to the low coverage of N_{ads} species.

After a helium purge (Fig. 3B), a new switch, He → 1% NO/1% Ar/He at 300 K, was performed (Fig. 3C) to quantify the amount of reversible adsorbed NO species, $Q\text{NO}_{wads} = 11$ µmol/g, that is consistent with the modifications of the IR bands of the molecularly adsorbed NO species during the helium purge (Fig. 1A). The amount of strongly adsorbed NO species, $Q\text{NO}_{sads} = 42$ µmol/g, is higher than $Q\text{CO}_{sads} = 34$ µmol/g, due to the formation of the NO_x–Al_2O_3 species. After a helium purge (Fig. 3D), a 1% CO/1% Ar/He mixture was introduced (Fig. 3E), revealing that a significant fraction of NO desorbed (in agreement with Fig. 1A) due to competitive chemisorption. The amount of CO adsorbed in Fig. 3E was 31 µmol/g (a value consistent with 34 µmol/g on a freshly reduced solid), and the amount of NO displaced was 23 µmol/g. The ratio 34/23 = 1.4 is consistent with the data on Pt single crystals [38] indicating saturation coverages for adsorbed CO and NO species of 0.75 and 0.5, respectively. In Fig. 3E, CO adsorption is associated with low CO_2 production, probably because of the reduction of strongly adsorbed oxygen species formed by the dissociation of NO.

3.4. Oxidation of the adsorbed CO species on Pt/Al_2O_3 solid for $D < 0.26$

For the development of the microkinetic study, the aforementioned FTIR and MS observations led to the conclusion that the competitive chemisorption CO–NO was in favor of CO. This indicates that NO could not displace the linear CO species at 300 K for short adsorption durations. However, NO could be dissociated on the free Pt° sites because of desorption of the bridged CO species, leading to a decreased amount of linear CO species by oxidation. According to the aims of the present study, and to prevent significant modification of the coverage of the linear CO species before the oxidation with O_2, the adsorption of NO was limited to a short duration.

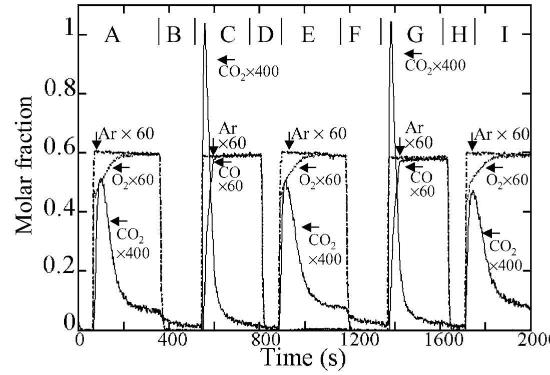

Fig. 4. CO_2 production at 300 K during oxidation/reduction cycles of the adsorbed species on 2.9% Pt/Al_2O_3 (after 3 previous cycles). (A, E, I) Oxidation stage with 1% O_2/1% Ar/He; (B, D, F, H) desorption in helium; (C, G) reduction stage with 1% CO/1% Ar/He.

3.4.1. Profile of $RCO_2(t)$ in the absence of N-containing species

The impact of the Pt dispersion on the rate of oxidation of the linear CO species has been described in detail for $D > 0.44$ [10,11]. Fig. 4 shows the CO_2 production for $D = 0.26$ during several O/R cycles, performed after three previous O/R cycles to saturate the Al_2O_3 surface with carbonate species [5,10,11]. In Fig. 4A, the switch He → 1% O_2/1% Ar/He, performed after a reduction step followed by a desorption in helium during 80 s, led to a rate of CO_2 production, $RCO_2(t)$, with no induction period, which is consistent with the fact that the bridged CO species desorbed significantly during the helium purge for $D < 0.5$ [10,11]; the $B(0)$ value does not fulfil the criterion (3). The amount of CO_2 production in Fig. 4A is 28 µmol/g whereas that of the O_2 consumption is 29 µmol/g. This finding indicates that oxidation of the linear CO species (denoted by L-CO), the main adsorbed CO species on the Pt surface, corresponds to the global reaction

$$\text{L-CO} + O_2 \rightarrow CO_2 + O_{sads}, \tag{5}$$

where O_{sads} is a strongly adsorbed oxygen species, in agreement with previous results for $D > 0.44$ [3]. Fig. 4C shows CO_2 production during reduction of the O_{sads} species formed in reaction (5), after a helium purge (Fig. 4B) to remove O_2, by the switch He → 1% CO/1% Ar/He. The initial rate was higher than that during the oxidation of the linear CO species (Fig. 4A), as observed previously for $D > 0.44$ [5]. The amount of CO_2 production shown in Fig. 4B is 27 µmol/g and that of CO consumption is 58 µmol/g, indicating that reduction of the O_{sads} species corresponds to the global reaction

$$O_{sads} + 2CO \rightarrow CO_2 + CO_{ads}. \tag{6}$$

One aim of the present experimental microkinetic study is to determine how CO_2 production from the oxidation of the adsorbed CO species is modified if NO is adsorbed before the oxidation stage.

3.4.2. Evolution of the coverage of the linear CO species during oxidation

MS observations provide the rate of CO_2 production from the oxidation of the linear and bridged CO species, whereas

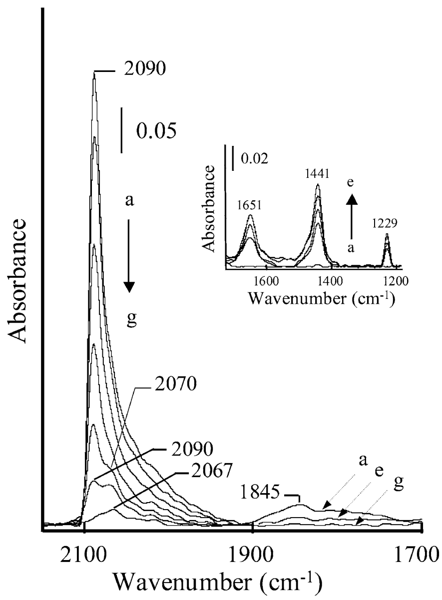

Fig. 5. FTIR spectra during the oxidation of the adsorbed CO species on a freshly reduced Pt/Al_2O_3 solid at 300 K: (a) in helium after CO adsorption; (b–g) time on stream in 1% O_2/He: 9, 17, 26, 35, 45, and 135 s, respectively.

FTIR data differentiate the two species. Fig. 5 shows the evolution of the IR bands of each adsorbed CO species on the freshly reduced Pt/Al_2O_3 solid ($D \approx 0.20$) with time on stream in 1% O_2/He. The IR band of the linear CO species at 2090 cm^{-1} decreased (Fig. 5, spectra a–g) without any shift associated with the disappearance of those of the bridged CO species in the 1900–1700 cm^{-1} range. In parallel, the IR bands of the carbonate species on the support at 1651, 1441, and 1229 cm^{-1} increased (Fig. 5, inset) due to adsorption of the CO_2 produced by reaction (5). The main difference from the observations on Pt/Al_2O_3 with a higher dispersion [2,10] is related to detection of the small IR band at ≈2070 cm^{-1} (Fig. 5), indicating a second linear CO species of low reactivity. The detection of several IR bands for linear CO species (i.e., linear CO species on steps and terraces) is due to the structure of the Pt particles, which is dependent on particle size and on the support [10,12, and references therein]. Curve □ in Fig. 6 shows the evolution of the coverage, θ_L, of the linear CO species (without differentiation of the two IR bands) with time on stream t in O_2, $\theta_L = A(t)/A(0)$, where $A(t)$ and $A(0)$ are the IR band area of the linear CO species at time t of oxidation. The coverage began to decrease at $t = 0$ s, consistent with (a) the decreasing exponential-like profile of the CO_2 production in Fig. 4A and (b) the fact that the linear CO species dominates CO adsorption. Successive O/R cycles provide the experimental data overlapping the curve □ in Fig. 6.

3.5. Impact of the adsorption of NO on the oxidation of the adsorbed CO species by MS

3.5.1. Adsorption of NO after CO adsorption

After the adsorption of CO (Fig. 2A) on the freshly reduced Pt/Al_2O_3 catalyst followed by a helium purge to decrease the amount of bridged CO species, adsorption of NO was performed (Fig. 2E) for a short period (80 s), to prevent significant oxidation of the linear CO species (Figs. 1B and 2E). Then, after a helium purge, a 1% O_2/1% Ar/He mixture was introduced to perform the oxidation of adsorbed CO species. Fig. 7A shows a $RCO_2(t)$ curve slightly modified by NO adsorption compared with that shown in Fig. 4A; a short induction period for oxygen consumption (the negative O_2 peak in Fig. 7A), $t_m = 12$ s, from the appearance of Ar can be seen. This indicates that NO adsorption/dissociation had only a limited impact on the oxidation rate of the adsorbed CO species. The amounts of O_2 consumed and CO_2 produced, 25 and 12 µmol/g, respectively, do not correspond to reaction (5) because a fraction of the CO_2 production is adsorbed on the alumina support. After a helium purge Fig. 7B), reduction of the O_{sads} by CO was performed (Fig. 7C). CO consumption was 43 µmol/g, and CO_2 production was 9 µmol/g, lower than that expected from reaction (6), due to (a) the adsorption of CO_2 on Al_2O_3 and (b) the fact that all of the O_{sads} species were not reduced during the first reduction stage [2–4]. Fig. 7C shows slight NO production

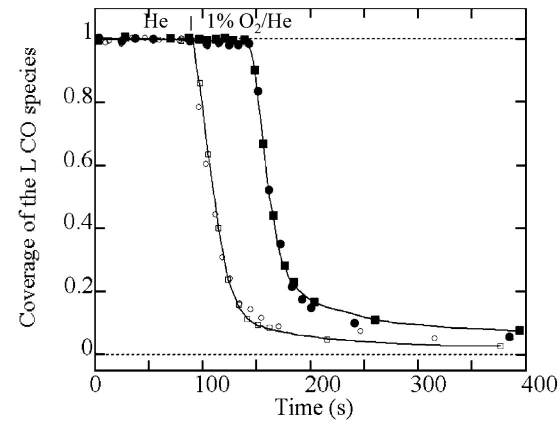

Fig. 6. Evolution of the coverage of the linear CO species during oxidation at 300 K with 1% O_2/He according to several experimental conditions: (□) after adsorption of 1% CO/He; (○) after 80 s of adsorption of NO following the reduction stage of the first O/R cycle; (■) oxidation during the second O/R cycle after curve ○; (●) oxidation during the third cycle after curve ■.

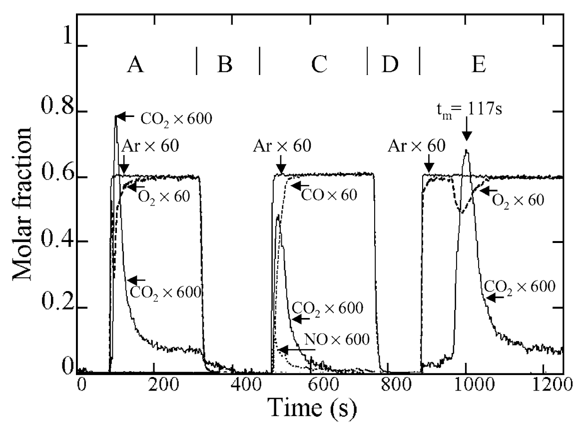

Fig. 7. Impact of the adsorption of NO at 300 K on the oxidation with 1% O_2/1% Ar/He of the adsorbed CO species on 2.9% Pt/Al_2O_3. (A) Oxidation stage following the adsorption of NO after adsorption of CO on a freshly reduced solid; (B, D) desorption in helium; (C) reduction stage in 1% CO/1% Ar/He; (E) oxidation stage in 1% O_2/1% Ar/He.

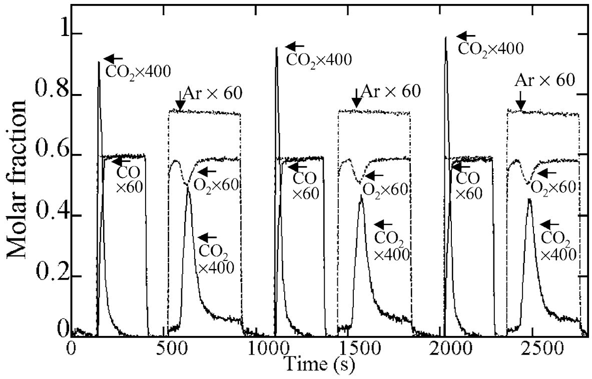

Fig. 8. CO_2 production during three O/R cycles of the adsorbed species on 2.9% Pt/Al_2O_3 after the adsorption of NO.

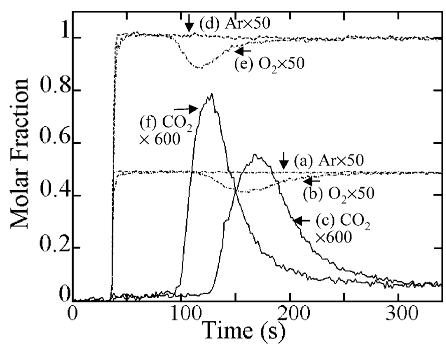

Fig. 9. Impact of the partial pressure of O_2 on the CO_2 production from the oxidation of the adsorbed CO species in the presence of N-containing adsorbed species: (a–c) oxidation with 1% O_2/1% Ar/He; (d–f) oxidation using 2% O_2/2% Ar/He.

(4 µmol/g), which may be due to competitive chemisorption between NO_x–Al_2O_3 (formed during the NO adsorption) and the carbonate species. After a helium purge (Fig. 7D), a new oxidation of the adsorbed CO species was performed (Fig. 7E). After this new oxidation, the $RCO_2(t)$ profile was strongly altered (compare Fig. 7E with Figs. 4A, 4E, and 4I), marked by a clear induction period with a CO_2 peak (23 µmol/g) with a maximum at $t_m = 117$ s measured from the appearance of Ar. This peak is associated with O_2 consumption (negative O_2 peak in Fig. 7E) of 20 µmol/g, in agreement with reaction (5), because the alumina support was saturated by the carbonate species during the experiments illustrated in Figs. 7A and 7C. Fig. 8 shows the observations during three successive O/R cycles after the oxidation shown in Fig. 7E with no new NO adsorption. An induction period similar to that shown in Fig. 7E ($t_m = 117$ s) can be observed during the oxidation stages. Fig. 8 clearly shows that the perturbations of the oxidation process by the adsorption/dissociation of NO were permanent during the O/R cycles at 300 K (they were suppressed by the reduction procedure at 713 K).

After a reduction procedure at 713 K, the experiments illustrated in Figs. 7 and 8 provided similar observations; however, their t_m values were never exactly the same. For instance, curve c in Fig. 9 shows that $t_m = 132$ s using 1% O_2/1% Ar/He. The difference between the t_m values for two successive experiments stems from the fact that in addition to the impact of NO adsorption, t_m is dependent on several kinetic parameters (Eq. (1)) that can be affected by slight differences in the experimental procedure [11]. The impact of the oxygen partial pressure, P_{O_2}, on t_m (after modification of the oxidation process by NO adsorption/dissociation) is shown in Fig. 9; this figure compares the evolution of the O_2 and CO_2 molar fractions using x% O_2/x% Ar/He with $x = 1$ and 2 for curves (b, c) and (e, f), respectively. It can be seen that the increase in P_{O_2} decreased t_m and increased $RCO_{2\,m}$, as was observed previously on Pt/Al_2O_3 catalysts with high Pt dispersion [11].

3.5.2. Preadsorption of NO

The adsorption of NO was performed for 3 min on freshly reduced Pt/Al_2O_3 solid; then, after a helium purge of 80 s, CO adsorption was performed, leading to desorption of the adsorbed NO species (Figs. 1A and 3E). After 80 s in helium, a 1% O_2/1% Ar/He mixture was introduced to perform the oxidation of the adsorbed CO species (results not shown). A large induction was observed, $t_m = 126$ s, which increased slightly after the second O/R cycle, $t_m = 154$ s, probably due to the presence of the O_{sads} species formed during the first oxidation. For $D > 0.6$, it has been observed that t_m augments during the three first O/R cycles (see Fig. 4 in [11]).

3.5.3. NO adsorption after the reduction stage of an O/R cycle

A fraction of the O_{sads} species formed according to reaction (5) during the first oxidation of the adsorbed CO species remained on the surface after the first reduction stage [5], leading to a Pt° surface different than that after adsorption of CO or NO on a freshly reduced solid. After the last reduction stage of three O/R cycles (shown in Fig. 4G), 1% NO/1% Ar/He was adsorbed for 80 s. After a helium purge, the oxidation with 1% O_2/1% Ar/He led to a small induction period: $t_m = 42$ s, similar to that shown in Fig. 7A. After the reduction stage, with 1% CO/1%Ar/He, the following oxidation stages led to $t_m = 178$ s, similar to that illustrated in Figs. 7E and 8. This demonstrated that the remaining fraction of O_{sads} species did not qualitatively modify the impact of NO; it is the duration of the induction period that was longer after the O/R cycles.

The aforementioned observations regarding modification of the $RCO_2(t)$ profile by the presence of a small amount of adsorbed N-containing species can be summarized as follows: (a) The adsorption/dissociation of NO after the formation of the linear and bridged CO species on the reduced 2.9% Pt/Al_2O_3 solid did not give a strong induction period ($t_m = 12$ s in Fig. 7A); (b) t_m was larger (42 s) when NO was adsorbed after the reduction stage of several O/R cycles; and (c) t_m was very large (in the range of 115–180 s) if the adsorption of CO follows the adsorption of NO (whatever the state of the Pt surface before the NO adsorption). This leads to the conclusion that a large induction period is not due to the simple poisoning of free Pt° sites by a small amount of strongly adsorbed N-containing species: it is linked to the impact of these species on the reactivity of the linear and bridged CO species.

3.6. *Modification of the oxidation of the adsorbed CO species by NO adsorption studied by FTIR*

FTIR observations provide additional data on the evolution of the coverages of the adsorbed species during the O/R cycles after NO adsorption. Moreover, an experiment can justify the presence of a small amount of strongly adsorbed N-containing species.

3.6.1. *Oxidation after adsorption NO on the adsorbed CO species*

After CO adsorption, three O/R cycles were performed (see Figs. 4 and 5); then, after the last reduction stage, 1% NO/He was adsorbed for 80 s (to limit the decrease in the IR band of the linear CO species). After a helium purge of 80 s, oxidation with 1% O_2/He led to a decrease in the IR band of the linear CO species (results not shown), providing the evolution of coverage θ_L with the duration of the oxidation according to curve ○ in Fig. 6. The overlap of curves ○ and □ indicates that the NO adsorption on the adsorbed CO species did not significantly disturb the oxidation of the linear CO species, in agreement with the findings shown in Fig. 7A. However, after a reduction stage with 1% CO/He, the following oxidation stage with 1% O_2/He led to curve ■ in Fig. 6: the coverage of the linear CO species decreased significantly only after a delay due to oxygen introduction at the difference of curves ○ and □. This delay corresponds to the induction period of the $RCO_2(t)$ curves in shown Fig. 8. The overlap of curves ■ and ● obtained after a second O/R cycle confirms that the perturbation of the oxidation process by the N-containing species is permanent at 300 K.

3.6.2. *On the presence of N-containing species after NO adsorption on the adsorbed CO species*

The FTIR spectra recorded after the adsorption of CO on a surface perturbed by the adsorption of NO do not reveal the presence of N-containing adsorbed species on the Pt° sites (Fig. 1A). This may be because they are not detectable by FTIR (small amounts or/and inactive in IR) or because perturbation by NO adsorption is linked to another process (e.g., surface reconstruction). The presence of N-containing species was revealed by the following experiment. After the adsorption of 1% NO/He at 300 K on the freshly reduced solid (Fig. 10a), followed by a helium purge of 80 s, a 1% CO/He mixture was introduced (Fig. 10b), leading to a spectrum similar to that shown in Fig. 1A. After a helium purge, the temperature was increased progressively to create temperature-programmed surface reactions (TPSRs) among the various adsorbed species (spectra c–e in Fig. 10). It can be observed that (a) new small IR bands at 2257 and 2233 cm^{-1} appeared at $T = 354$ K and increased progressively up to $T = 415$ K, and (b) in parallel, the IR bands of the adsorbed CO species decreased. According to literature data, the IR bands at 2257 and 2233 cm^{-1} must be ascribed to strongly adsorbed isocyanate species on the alumina support via diffusion from the Pt particles and to either adsorption on the Pt° particles or a negatively charged isocyanate species, respectively [19,43,44]. Detection of the isocyanate species provides clear proof that N-containing species

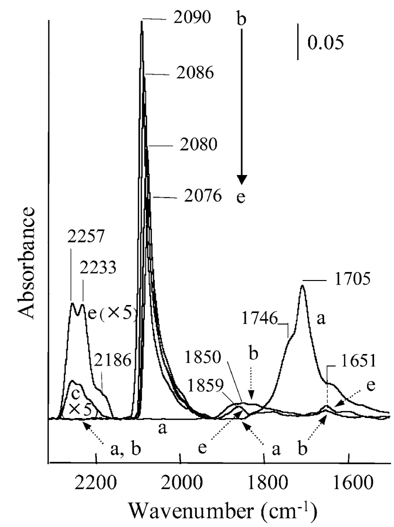

Fig. 10. On the presence of a small amount of N-containing adsorbed species in the presence of adsorbed CO species on the Pt surface by using FTIR experiments. (a) Adsorption of 1% NO/He at 300 K on the freshly reduced Pt/Al_2O_3 solid; (b) adsorption of 1% CO/He at 300 K after (a); (c–e) TPSR in helium after (b) at 354, 391, and 415 K, respectively.

were co-adsorbed with the linear and bridged CO species after NO adsorption. Their formation may have involved either N_{ads} species or an inactive molecular NO species [45]. The IR bands of the isocyanate species in Fig. 10 are very weak, indicating the presence of a small amount of N-containing species; for example, they increased by a factor ≈100 after 15 min of 0.5% NO/0.5% CO/He at 553 K (result not shown). This is consistent with the fact that these bands could form only on the Pt° sites adsorbing the bridged CO species, which represent <8% of the total number of Pt° sites. Note that the coverage of the linear CO species at $T = 415$ K during TPSR was slightly smaller in Fig. 10 ($\theta_L \approx 0.7$) than during a simple TPD ($\theta_L = 0.8$) [46]. This suggests that several processes contributed to the decrease in the amount of linear CO species during the TPSR illustrated in Fig. 10, including (a) its desorption [46], (b) its reaction to form isocyanate species, and (c) its oxidation via strongly adsorbed oxygen species formed by NO dissociation at 300 K.

4. Discussion

4.1. *On the nature of the N-containing adsorbed species after CO adsorption*

Fig. 10 clearly shows that N-containing adsorbed species were co-adsorbed with the linear and bridged CO species after NO adsorption. The main experimental fact is that the perturbation of the oxidation of the adsorbed CO species created by these species was permanent at $T < 350$ K (Fig. 8), indicating that they were neither displaced nor transformed by CO and O_2. Figs. 1–3 show that the competitive chemisorption of CO and NO at 300 K for the molecularly adsorbed species was in favor of CO. These observations are consistent with the findings of Pt single-crystal studies that found only adsorbed CO species during co-adsorption of CO and NO at 300 K [23,24].

The fact that the linear CO species displaced the linear NO species on the present Pt/Al_2O_3 catalyst is in agreement with their respective heats of adsorption E_θ at a coverage θ determined in previous works: $E_0 = 206$ and $E_1 = 115$ kJ/mol for the linear CO species [7,8] and $E_0 = 135$ and $E_1 = 105$ kJ/mol for the linear NO species [18]. The situation is different for the bridged CO species because the E_θ values for $D < 0.5$, $EB_0 = 94$ and $EB_1 = 45$ kJ/mol, [8] are smaller than those of the linear NO species [18] and significantly smaller than literature data on the bridged NO species. Yeo et al. [38] determined by single-crystal microcalorimetry that the heat of adsorption of NO at low coverage on a Pt single crystal, corresponding to the bridged NO species, was >200 kJ/mol, consistent with the results of DFT calculations [21,22]. However, the increase in θ leads to reconstruction of the surface, favoring the linear NO species [38]. The aforementioned findings lead us to adopt the view that the N-containing species remaining on the Pt surface after O/R cycles is not a molecularly adsorbed NO species but rather is probably a N_{ads} species formed by the dissociation of NO.

This NO dissociation is supported by the slow (compared with O_2) oxidation of the adsorbed CO species at 300 K (Figs. 1–3), involving the Pt° sites released by desorption of the bridged CO species. This could not be sustained at 300 K in the absence of adsorbed CO species. DFT calculations [21] considering NO dissociation on the step sites of Pt(211) indicate that the transition state for the dissociation had lower energy (by 64 kJ/mol) than NO_g, supporting the view that NO could be dissociated on those sites via the formation of a bridged NO species with a heat of adsorption of 228 kJ/mol. The heats of adsorption of N_{ads} and O_{ads} species would be expected to be higher, leading to the conclusion that NO dissociation is overall an energetically favored process [21]. A recent DFT study [39] confirmed these views, showing that whatever the nature of the Pt sites, the binding energies of N_{ads} (>3.9 eV) and O_{ads} (>3.2 eV) were higher than the binding energy of NO (>1.3 eV), indicating that N_{ads} could remain on a Pt° surface. This is consistent with the STM observations of Zambelli et al. on Ru(0001) [40,41] showing that NO dissociated at 300 K on the step sites and the N_{ads} species did not desorb, but rather migrated to the terrace sites. These observations have been supported by DFT calculations and they seem to be valid for other metal surfaces as well [42]. The nature of the defect sites may lead to different conclusions concerning the stability of the N_{ads} species from DFT calculations [37,42]. The stability of N_{ads} at 300 K on a Pt surface is supported by the TPD study of Mukerji et al. [30] after adsorption of NO at 300 K. Those authors reported that strongly adsorbed NO_{ads} and N_{ads} species formed at a low temperature reacted at 471 K to form N_2O_{ads} that either desorbed as N_2O or was decomposed into N_2 and O_{ads}. The foregoing discussion supports the view that the N_{ads} species formed by the NO dissociation at 300 K on the Pt° sites adsorbing the bridged CO species can be eliminated only by reaction at a higher temperature, such as the formation of isocyanate species during TPSR (Fig. 10). This explains the permanent perturbation of the oxidation of the adsorbed species by NO adsorption/dissociation at 300 K.

4.2. *Impact of NO adsorption on the induction period observed on $RCO_2L(t)$*

Expressions (1) and (2) are used to support the interpretations of the induction period during oxidation of the adsorbed CO species in the presence of co-adsorbed N-containing species (Figs. 7–9). In the absence of NO adsorption, $RCO_2(t)$ had a decreasing exponential-like profile because the $B(0)$ value did not obey the criterion specified in (3). The first observation is that the adsorption of NO after that of CO on the freshly reduced solid created a very small induction ($t_m = 12$ s) during the subsequent oxidation stage (Fig. 7A). This means that the criterion (3) was fulfilled after NO adsorption. This change cannot be ascribed to an increase in $B(0)$, because NO adsorption can only decrease $B(0)$ due to oxidation of the bridged CO species via the NO dissociation or to competitive chemisorption. The $B(0)$ value fulfilled the criterion in (3) after NO adsorption due to the decreased value of the right side of expression (3). For instance, the formation of N_{ads} on the Pt° sites released by desorption of the bridged CO species either decreased NT_B or increased the ratio k_{OB}/k_3. We show below that the activation energy of oxidation of the bridged CO species was increased after NO adsorption (decrease in k_{OB}).

The main impact of NO adsorption/dissociation was observed after the readsorption of CO during the first reduction step (Fig. 7C). Fig. 7E shows that this situation entailed a strong induction period and that this modification was irreversible during the subsequent O/R cycles at 300 K (Fig. 8). Clearly, the induction period was linked to the adsorption of CO on a Pt surface perturbed by the presence of the N-containing species; the criterion (3) was largely fulfilled. Considering previous work [10,11], this must be due to the increased heat of adsorption of the bridged CO species due to the presence of N_{ads}. This led to a larger amount of bridged CO species for the same desorption period ($t_d = 80$ s) before the oxidation stage; the $B(0)$ value was higher than that without N_{ads} species, fulfilling criterion (3). This was confirmed by a subsequent experiment; after several O/R cycles performed on a surface perturbed by the N_{ads} species (Fig. 8), the increased duration of the desorption t_d before oxidation from 80 s to 50 min led to a significantly lower

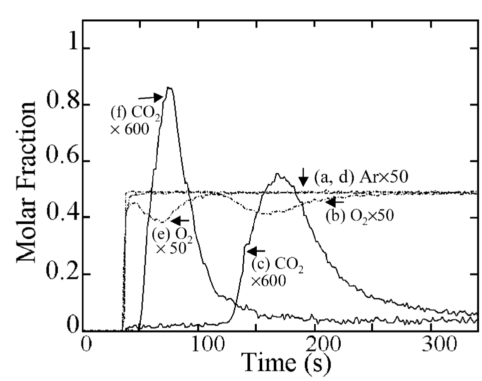

Fig. 11. Impact of the desorption duration t_d in helium after the CO adsorption on the CO_2 production from the oxidation of the adsorbed CO species, using 1% O_2/1% Ar/He, in the presence of N_{ads} species. (a–c) $t_d = 80$ s; (d–f) $t_d = 50$ min.

value of t_m, as shown in Fig. 11 (compare curves c and f). This decrease is due to the decrease in $B(0)$ linked to the long desorption duration; there are more Pt° sites for the activation of oxygen at time $t = 0$. Note that the next O/R cycle after curve f in Fig. 11, using a helium purge of 80 s, provides an induction period similar to curve c in Fig. 11. This demonstrates that the long desorption period did not significantly modify the amount of N_{ads} species.

The kinetic model developed for the interpretation of the induction period on Pt/Al_2O_3 catalysts with high Pt dispersions can be verified by noting that the impact of oxygen partial pressure on the experimental values of t_m and RCO_2L_m corresponded to what was expected based on expressions (1) and (2) [11]. Similar experiments were performed to determine whether the same kinetic model could be applied for the observations in the presence of co-adsorbed N_{ads} and CO species. Fig. 9 shows that decreasing P_{O_2} by a factor of 2 increased t_m by a factor of (132 s/91 s) = 1.45 and decreased $RCO_{2\,m}$ by a factor of (1/1.46), as was expected based on expressions (1) and (2): $\sqrt{2}$ and $(1/\sqrt{2})$, respectively. This confirms that the co-adsorbed N_{ads} species did not change the nature of the elementary steps of the kinetic model involved in the oxidation of the linear CO species [11], but only modified the kinetic parameters of some elementary steps.

In a previous work [11], we showed that t_m decreases with increasing oxidation temperature, T, and that $\ln t_m = f(1/T)$ is a straight line, as observed by Zhou and Gulary [16] on Pd/Al_2O_3 catalysts. Expression (1) indicates that the slope of the straight line provides $E_{OB} - (E_{O_2}/2)$, where E_{OB} is the activation energy of oxidation of the bridged CO species and E_{O_2} is the heat of adsorption of the weakly adsorbed oxygen species involved in the oxidation at low temperatures [11]. We have studied the evolution of t_m with an oxidation temperature of $T < 350$ K to limit the modifications of the impact of N_{ads} (formation of the isocyanate species at $T > 350$ K in Fig. 10). Fig. 12 shows $\ln t_m = f(1/T)$ as a straight line, confirming that the kinetic model developed previously [11] remained operative after the adsorption/dissociation of NO. However, the slope of the straight line indicates that $E_{OB} - (E_{O_2}/2) = 57$ kJ/mol, whereas it was equal to 44 kJ/mol before NO adsorption [11]. This increase may be due either to the augmentation of E_{OB} (k_{OB} decreases) or to the decrease in E_{O_2}.

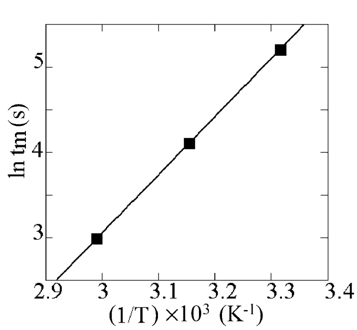

Fig. 12. Impact of the oxidation temperature on t_m according to $\ln(t_m) = f(1/T)$.

5. Conclusion

The present study confirms that the experimental microkinetic approach of a catalytic process such as the CO/O_2 reaction on Pt/Al_2O_3 catalysts is a powerful tool for establishing a relationship between the changes of a macroscopic kinetic parameter (such as TOF [6,14] and the rate of O_2 oxidation of the adsorbed CO species, $RCO_2(t)$ [11]) and the kinetic parameters of the elementary steps. We have explained how co-adsorbed N_{ads} species affects $RCO_2(t)$. We have shown that NO can be adsorbed/dissociated on the Pt° sites released by desorption of the bridged CO species that represents a small fraction of the Pt° sites adsorbing CO. This leads to a $RCO_2(t)$ curve with an induction period characterized by the coordinates of its maximum: t_m, $RCO_{2\,m}$, whereas a decreasing exponential-like profile is observed in the absence of N_{ads} species. This induction period is due mainly to the altered heat of adsorption of the bridged CO species in the presence of the N_{ads}. The modifications of the rate constants of oxidation of the linear and bridged CO species also contribute to the induction period. Our results reinforce the previously expressed view [2–6] that two types of Pt° sites are involved in the CO/O_2 reaction at low temperature.

Finally, the study has shown that the kinetic parameters controlling the rate of the CO/O_2 reaction can be modified in the presence of co-adsorbed species using complex gas mixtures such as $CO/NO/O_2$, corresponding to three-way and De-NO_x catalytic processes similar to their modifications due to Pt dispersion [11]. It must be noted that the decreased rate of oxidation of the adsorbed CO species by co-adsorbed N-containing species described in the present study is consistent with the inhibition of the CO/O_2 reaction on Pt/Al_2O_3 by NO observed by Voltz et al. [47].

Acknowledgments

The authors thank RENAULT, SAS for financial support and MENRT (Ministère de l'Education Nationale, de la Recherche et de la Technologie) for a doctoral research fellowship (S.D.).

References

[1] J.A. Dumesic, D.F. Rudd, L.M. Aparicio, J.E. Rekoske, A.A. Trevino, The Microkinetics of Heterogeneous Catalysis, ACS Prof. Ref. Book, American Chemical Society, Washington, DC, 1993.
[2] A. Bourane, D. Bianchi, J. Catal. 202 (2001) 34.
[3] A. Bourane, D. Bianchi, J. Catal. 209 (2002) 114.
[4] A. Bourane, D. Bianchi, J. Catal. 209 (2002) 126.
[5] A. Bourane, D. Bianchi, J. Catal. 220 (2003) 3.
[6] A. Bourane, D. Bianchi, J. Catal. 222 (2004) 499.
[7] O. Dulaurent, D. Bianchi, Appl. Catal. 196 (2000) 271.
[8] A. Bourane, O. Dulaurent, D. Bianchi, J. Catal. 196 (2000) 115.
[9] A. Bourane, D. Bianchi, J. Catal. 218 (2003) 447.
[10] A. Bourane, S. Derrouiche, D. Bianchi, J. Catal. 228 (2004) 288.
[11] S. Derrouiche, D. Bianchi, J. Catal. 230 (2005) 359.
[12] P. Pillonel, S. Derrouiche, A. Bourane, F. Gaillard, P. Vernoux, D. Bianchi, Appl. Catal. 278 (2005) 223.
[13] M. Boudart, Catal. Lett. 65 (2000) 1.
[14] G.S. Zafiris, R.J. Gorte, J. Catal. 140 (1993) 418.
[15] S.M. Dwyer, C.O. Bennett, J. Catal. 75 (1982) 275.
[16] X. Zhou, E. Gulari, Langmuir 2 (1986) 709.

[17] Y. Li, D. Boecker, R.D. Gonzalez, J. Catal. 110 (1988) 319.
[18] A. Bourane, O. Dulaurent, S. Salasc, C. Sarda, C. Bouly, D. Bianchi, J. Catal. 204 (2001) 77.
[19] K.I. Hadjiivanov, Catal. Rev. Sci. Eng. 42 (2000) 71.
[20] W.A. Brown, R.K. Sharma, D.A. King, J. Phys. Chem. B 102 (1998) 5303.
[21] R.J. Mukerji, A.S. Bolina, W.A. Brown, Z.P. Liu, P. Hu, J. Phys. Chem. B 108 (2004) 289.
[22] H. Orita, I. Nakamura, T. Fujitani, J. Phys. Chem. B 109 (2005) 10312.
[23] J.H. Miners, P. Gardner, D.P. Woodruff, Surf. Sci. 547 (2003) 355.
[24] P. Gardner, R. Martin, M. Tushaus, A.M. Bradshaw, Surf. Sci. 269 (1992) 405.
[25] P.T. Fanson, W.N. Delgass, J. Lauterbach, J. Catal. 204 (2001) 35.
[26] D. Bianchi, T. Chafik, M. Khalfallah, S.J. Teichner, Appl. Catal. A 105 (1993) 223.
[27] W.A. Brown, D.A. King, J. Phys. Chem. B 104 (2000) 2578.
[28] W.F. Banholzer, R.I. Masel, J. Catal. 85 (1984) 127.
[29] Q. Ge, M. Neurock, J. Am. Chem. Soc. 126 (2004) 1551.
[30] R.J. Mukerji, A.S. Bolina, W.A. Brown, J. Chem. Phys. 119 (2003) 10844.
[31] G. Pirug, H.P. Bonzel, H. Hopster, H. Ibach, J. Chem. Phys. 71 (1979) 593.
[32] B.A. Morrow, J.P. Chevrier, L.E. Moran, J. Catal. 91 (1985) 208.
[33] D.R. Lide (Ed.), Handbook of Chemistry and Physics, CRC Press, Boca Raton, FL, 2001.
[34] T. Maunula, J. Ahola, T. Salmi, H. Haario, M. Harkonen, M. Luoma, V.J. Pohjola, Appl. Catal. B 12 (1997) 287.
[35] R. Burch, S.T. Daniells, P. Hu, J. Chem. Phys. 117 (2002) 2902.
[36] R. Burch, S.T. Daniells, P. Hu, J. Chem. Phys. 121 (2004) 2737.
[37] A. Eichler, J. Hafner, J. Catal. 204 (2001) 118.
[38] Y.Y. Yeo, L. Vattuone, D.A. King, J. Chem. Phys. 104 (1996) 3810.
[39] D.C. Ford, Y. Xu, M. Mavrikakis, Surf. Sci. 587 (2005) 159.
[40] T. Zambelli, J. Trost, J. Wintterlin, G. Ertl, Phys. Rev. Lett. 76 (1996) 795.
[41] T. Zambelli, J. Wintterlin, J. Trost, G. Ertl, Science 273 (1996) 1688.
[42] B. Hammer, Phys. Rev. Lett. 83 (1999) 3681.
[43] V.A. Matyshak, O.V. Krylov, Catal. Today 25 (1995) 1.
[44] J. Rasko, J. Kiss, Appl. Catal. A 298 (2006) 115.
[45] F. Solymosi, J. Sarkany, A. Schauer, J. Catal. 46 (1977) 297.
[46] A. Bourane, O. Dulaurent, K. Chandes, D. Bianchi, Appl. Catal. A 214 (2001) 193.
[47] S.E. Voltz, C.R. Morgan, D. Liederman, S.M. Jacob, Ind. Eng. Chem. Prod. Res. Dev. 12 (1973) 294.